

Characterization of peptide O $\cdots$ HN hydrogen bonds via  
multidimensional  $^1\text{H}$ -detected  $^{15}\text{N}/^{17}\text{O}$  solid-state nuclear magnetic  
resonance spectroscopy

Ivan Hung,<sup>a\*</sup> Wenping Mao,<sup>a</sup> Eric G. Keeler,<sup>b†</sup> Robert G. Griffin,<sup>b</sup> Peter L. Gor'kov,<sup>a</sup> Zhehong  
Gan<sup>a</sup>

<sup>a</sup> National High Magnetic Field Laboratory  
1800 East Paul Dirac Drive  
Tallahassee, Florida 32310  
USA

<sup>b</sup> Department of Chemistry and Francis Bitter Magnet Laboratory  
Massachusetts Institute of Technology  
Cambridge, Massachusetts 02139  
USA

<sup>†</sup> Current address: New York Structural Biology Center  
89 Convent Avenue  
New York, New York 10027  
USA

\* *Corresponding author e-mail:* hung@magnet.fsu.edu

## ABSTRACT

Solid-state NMR methods with high resolution and sensitivity are presented for identification and characterization of hydrogen-bonded  $^{15}\text{N}/^{17}\text{O}$  atomic pairs in peptide samples. Indirect  $^1\text{H}$  detection under fast magic-angle spinning, and the stronger  $^1\text{H}$ - $^{15}\text{N}$  and  $^1\text{H}$ - $^{17}\text{O}$  couplings are leveraged to significantly improve sensitivity over previous methods that use direct  $^{15}\text{N}$ - $^{17}\text{O}$  interactions.

*Keywords:*  $^{17}\text{O}$ ,  $^{15}\text{N}$ , hydrogen-bond, multidimensional NMR, distance measurement,  $^1\text{H}$  detection, solid-state NMR

The use of solid-state NMR spectroscopy to determine the structure of proteins largely revolves around the detection of spin  $I = 1/2$  nuclei such as  $^1\text{H}$ ,  $^{13}\text{C}$ , and  $^{15}\text{N}$ . Though equally important to protein structure, study of oxygen sites by NMR has in comparison been scarce since the only NMR-active isotope of oxygen,  $^{17}\text{O}$ , has a quadrupolar spin  $S = 5/2$  nucleus, low natural abundance (0.037%), and a low resonance frequency (5.772 MHz/T). These properties lead to a considerably lower sensitivity and resolution for NMR of  $^{17}\text{O}$  nuclei compared to  $^1\text{H}$ ,  $^{13}\text{C}$ , and  $^{15}\text{N}$ , and is further complicated by the high cost of  $^{17}\text{O}$  isotopic enrichment. However, the large shift range and quadrupolar interaction make  $^{17}\text{O}$  a sensitive probe of its structural and bonding environment,<sup>1</sup> and thus a desirable target of study. As a recent example,<sup>2</sup>  $^{17}\text{O}$  NMR spectroscopy was used to demonstrate that the dimeric symmetry of the gramicidin A ion channel is broken by differences in hydrogen-bonding to the water wire in the channel. For decades this asymmetry had been undetected using  $^{13}\text{C}$  and  $^{15}\text{N}$  NMR spectroscopy.

For uniformly  $^{17}\text{O}$ -enriched macromolecules, it is essential to incorporate  $^{17}\text{O}$  into the suite of multidimensional  $^1\text{H}/^{13}\text{C}/^{15}\text{N}$  NMR experiments<sup>3,4</sup> developed for sequential assignment of peptide residues and identification of long-range contacts, including hydrogen-bonds, for structural characterization. In this vein, high-resolution  $^1\text{H}/^{13}\text{C}/^{17}\text{O}$  multidimensional NMR

experiments have recently been reported via a combination of fast magic-angle spinning (MAS), indirect  $^1\text{H}$  detection, high  $^{17}\text{O}$  isotopic enrichment, and high magnetic fields.<sup>5</sup> This Communication complements and extends the previous work by demonstrating the use of multidimensional  $^1\text{H}/^{15}\text{N}/^{17}\text{O}$  NMR experiments as a facile method to identify hydrogen-bonded  $^{15}\text{N}$ - $^{17}\text{O}$  pairs in fully isotopically-enriched peptide samples, and measure the  $^1\text{H}$ - $^{17}\text{O}$  distance in the hydrogen bonds. As such, these methods can aid protein secondary (or tertiary) structure determination by pinpointing inter-residue proximities, as well as measure hydrogen-bond strength.

The low resonance frequencies of  $^{15}\text{N}$  and  $^{17}\text{O}$  nuclei (4.314 and 5.772 MHz/T, respectively) give rise to dipolar couplings of less than 100 Hz for internuclear distances greater than 2.5 Å. Therefore, correlation between the  $^{15}\text{N}$  and  $^{17}\text{O}$  nuclei across a hydrogen-bond by direct polarization transfer (Fig. 1a, grey dashed arrow) is rather inefficient. Instead of using the  $^{15}\text{N}$ - $^{17}\text{O}$  coupling, the approach used here takes advantage of the well-established hNH experiment utilizing the stronger dipolar couplings with protons,<sup>6,7</sup> which is a staple of  $^1\text{H}$ -detected methods employed under fast MAS<sup>3,4</sup> (*upper* and *lower* case letters denote nuclei that respectively *are* or *are not* observed during the path of polarization transfer used in the pulse sequence). Two-dimensional (2D) hNH spectra are used primarily to correlate the  $^1\text{H}$  and  $^{15}\text{N}$  nuclei of amide sites, as exemplified by the spectrum of N-acetyl-[U- $^{13}\text{C}$ ,  $^{15}\text{N}$ , 70%- $^{17}\text{O}$ ]-L-valyl-L-leucine (N-Ac-VL) in Fig. 1b (green). For reference, a 2D  $^{17}\text{O} \rightarrow ^1\text{H}$  CP spectrum (blue) is also shown, which displays the three distinct  $^{17}\text{O}$  sites in the sample: the Val amide site ( $\text{V}^{\text{NCO}}$ ), and the Leu protonated ( $\text{L}^{\text{COH}}$ ) and unprotonated ( $\text{L}^{\text{CO}}$ ) carboxylate oxygen sites.

Before proceeding further, it is worth summarizing two observations that are of relevance here from the previous  $^1\text{H}/^{13}\text{C}/^{17}\text{O}$  work:<sup>5</sup> 1. fast MAS makes efficient cross-polarization (CP)

between quadrupolar and  $I = 1/2$  nuclei more amenable due to improved accessibility to the  $n = 1$  double-quantum CP condition,<sup>8</sup> and 2. the use of  $^{17}\text{O}$  (in contrast to  $^1\text{H}$ ) as the source of initial polarization can provide better sensitivity due to the much shorter  $^{17}\text{O}$  longitudinal  $T_1$  relaxation, as observed for N-Ac-VL. Hence, an efficient method to correlate hydrogen-bonded  $^{15}\text{N}$  and  $^{17}\text{O}$  nuclei is to start from  $^{17}\text{O}$  polarization by preceding the hNH experiment with  $^{17}\text{O} \rightarrow ^1\text{H}$  CP (Fig. S1, ESI); thus, using the polarization transfer pathway schematized by the magenta arrows in Fig. 1a, i.e.,  $^{17}\text{O} \rightarrow ^1\text{H} \rightarrow ^{15}\text{N} \rightarrow ^1\text{H}$ . The advantage of taking this route is that the  $^1\text{H}$ - $^{17}\text{O}$  and  $^1\text{H}$ - $^{15}\text{N}$  dipolar couplings are typically at least an order of magnitude greater ( $> 1000$  Hz) than the direct coupling between  $^{17}\text{O}$  and  $^{15}\text{N}$  nuclei ( $< 100$  Hz). Thus, a much more sensitive and efficient transfer of polarization can be achieved over longer distances, while at the same time leveraging the sensitivity advantage of  $^1\text{H}$  detection under fast MAS. These spectra filter out all resonances except for NH groups with H atoms proximate to  $^{17}\text{O}$  nuclei, in effect selecting  $\text{O}\cdots\text{HN}$  hydrogen-bonded moieties. This is exemplified by the 2D NH and OH planes of the N-Ac-VL 3D OhNH spectrum shown in Fig. 1b (magenta), wherein the presence of a hydrogen-bond between the Val amide nitrogen atom ( $\text{V}^{\text{N}}$ ) and the unprotonated Leu carboxyl oxygen ( $\text{L}^{\text{CO}}$ ) is readily observed, in accordance with the X-ray crystal structure.<sup>9</sup>

The  $^{17}\text{O}$  resonances in Fig. 1b display broad ridges rather than sharp peaks due to the presence of second-order quadrupolar broadening. For a relatively small molecule such as N-Ac-VL, the  $^{17}\text{O}$  sites are well-resolved at a field of 18.8 T even in the presence of such broadening. However, the site resolution decreases substantially as the number of  $^{17}\text{O}$ -labeled residues increases, so it is desirable to obtain sharp isotropic  $^{17}\text{O}$  peaks. This can be achieved by averaging the quadrupolar broadening using the multiple-quantum MAS (MQMAS) method.<sup>10</sup> Here, the split- $t_1$  cos-1pMQMAS sequence is used to obtain a 2D  $\bar{\text{O}}\text{H}$  spectrum (Fig. 1c) with

sharp  $^{17}\text{O}$  peaks for all three oxygen sites (the overbar on the O is used to denote isotropic evolution), as also demonstrated before for  $^1\text{H}/^{13}\text{C}/^{17}\text{O}$  experiments.<sup>5</sup> Notably, the measured cos-  
lpMQMAS efficiency is ~25%, resulting in approximately equal signal-to-noise ratios between the  $\bar{\text{O}}\text{H}$  and  $\text{OH}$  spectra due to the concentration of signal into much sharper  $^{17}\text{O}$  resonances in the former. The fully evolved isotropic  $^{17}\text{O}$  dimension yields line widths of ~80-120 Hz. This high efficiency enables acquisition of 3D  $\bar{\text{O}}\text{hNH}$  spectra (pulse sequence in Fig. S2, ESI). Each peak in such a 3D spectrum (Fig. 1c, magenta) represents a single  $\text{O}\cdots\text{HN}$  hydrogen-bonded moiety, as also evidenced by the single peak in the 1D projection to  $^1\text{H}$  dimension arising from the only  $^{15}\text{N}\text{-}^1\text{H}\cdots^{17}\text{O}$  proximity in the sample. Thus, a sensitive and high-resolution method is obtained that readily selects hydrogen-bonded pairs of  $^{15}\text{N}\text{-}^{17}\text{O}$  nuclei. This method holds significant potential to aid protein structure determination without the necessity for selective  $^{17}\text{O}$  isotopic labelling, which as of today remains costly for general applications.

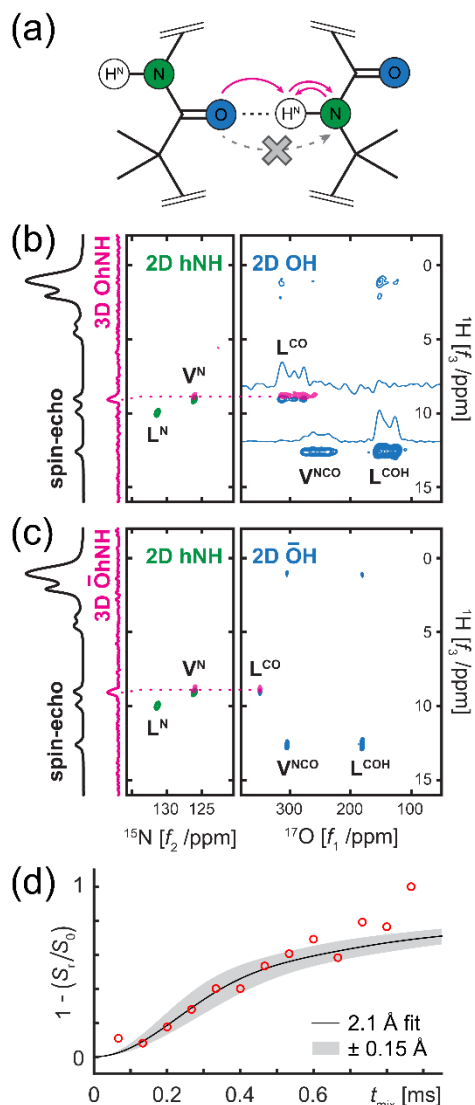


**Fig. 1.** (a) Schematic of a O...HN hydrogen-bond between two peptide residues showing the polarization transfer steps used in the 3D OhNH experiment (magenta arrows) in comparison to the much less effective direct transfer between  $^{17}\text{O}$  and  $^{15}\text{N}$  nuclei (grey dashed arrow). (b) Overlay of 2D NH and OH planes from a 3D OhNH spectrum (magenta) with 2D hNH (green) and OH (blue) spectra, showing the selection of hydrogen-bonded  $^{15}\text{N}/^{17}\text{O}$  pairs. (c) Same as (b), but using isotropic  $^{17}\text{O}$  evolution to improve site resolution. Isotropic  $^{17}\text{O}$  evolution in (c) is achieved using cos-1pMQMAS and split- $t_1$  acquisition with a factor  $k = 19/12$  for spin  $S = 5/2$  nuclei. The OhNH and  $\bar{\text{O}}\text{hNH}$  contour plots are offset vertically to aid the eye. (d)  $\{^1\text{H}\}^{17}\text{O}$  RESPDOR build-up curve for the Val NH resonance obtained using the  $^1\text{H}$ -detected ohNH $\{^{17}\text{O}\}$  pulse sequence. Total experimental times in hours for the spectra were (b) 3.4 for 2D hNH, 0.3 for 2D OH, 11.8 for 3D OhNH, (c) 0.3 for 2D  $\bar{\text{O}}\text{H}$ , 15.4 for 3D  $\bar{\text{O}}\text{hNH}$ , and 7.7 for ohNH $\{^{17}\text{O}\}$ .

In addition to identification of hydrogen-bonded  $^{15}\text{N}/^{17}\text{O}$  sites, the polarization transfer pathway used for the OhNH experiments can also be used to measure the hydrogen-bond  $^1\text{H}$ - $^{17}\text{O}$

distance. The O-H distance can serve as a measure of hydrogen-bond strength since the N-H bond length is relatively invariant in protein amide groups.<sup>11-13</sup> The measurement can be carried out by appending the well-established RESPDOR method<sup>14</sup> to the OhNH pulse sequence. The resulting experiment is denoted as ohNH<sup>{O}</sup> (Fig. S3, ESI), where the superscript {O} is used to represent the nucleus to which the detected H nuclei are recoupled to for distance measurement. In this experiment a series of O $\cdots$ HN filtered 2D hNH spectra is acquired with ( $S_r$ ) and without ( $S_0$ ) a  $^{17}\text{O}$  saturation pulse while varying the  $^1\text{H}$  heteronuclear dipolar recoupling time ( $t_{\text{mix}}$ ). The NH peak intensity at a series of  $t_{\text{mix}}$  is then plotted as a ratio  $(1 - S_r/S_0)$ , as shown for N-Ac-VL in Fig. 1d. By taking this ratio, effects from  $T_2$  relaxation are cancelled and a 'build-up' curve results that can be fitted analytically using Bessel functions to obtain the  $^1\text{H}$ - $^{17}\text{O}$  dipolar coupling, and consequently the internuclear distance.<sup>15,16</sup> Fig. 1d shows a fit of the RESPDOR curve which yields a distance of  $\sim 2.1$  Å between the Leu CO oxygen and Val NH proton. The NMR result agrees well with the distance of 1.97 Å obtained from X-ray diffraction<sup>9</sup> considering that distances measured by solid-state NMR are known to typically be longer due to atomic vibrations that are present at ambient temperatures, but absent at the lower temperatures used for X-ray crystallography.<sup>17</sup> Notably, the above method ensures that only NH peaks that have a nearby  $^{17}\text{O}$  sites appear in the hNH spectra. The distance measurement can also be performed by discarding the initial  $^{17}\text{O} \rightarrow ^1\text{H}$  CP portion of the pulse sequence and replacing it with a simple excitation pulse on the  $^1\text{H}$  channel to yield higher sensitivity. In that instance all NH peaks show up in the 2D hNH spectra without filtering for O $\cdots$ HN sites. To avoid interference from these signals to the RESPDOR curve, the peak of interest for O-H distance measurement needs to be well resolved.

There are a number of reports in the literature on the application of  $^{17}\text{O}$  NMR for the study of peptide and amino acid samples,<sup>1,18,19</sup> but to the best of our knowledge, there have only been a few using a combination of  $^{15}\text{N}$  and  $^{17}\text{O}$  nuclei.<sup>20-22</sup> These reports have all been performed with  $^{15}\text{N}$  or  $^{17}\text{O}$  observation at slower sample spinning frequencies, and employed the direct  $^{15}\text{N}$ - $^{17}\text{O}$  dipolar coupling for spectral correlation or distance measurement between the two nuclei. The experiments have generally shown relatively poor sensitivity since both the dipolar coupling and NMR receptivity depend on the nuclear resonance frequencies, i.e., their gyromagnetic ratios  $\gamma$ . The current work significantly improves upon the sensitivity by using indirect  $^1\text{H}$  detection under fast sample spinning, and ' $^1\text{H}$ -relayed'  $^{15}\text{N} \leftrightarrow ^{17}\text{O}$  polarization transfer. The former provides a sensitivity enhancement due to the higher  $^1\text{H}$  Larmor frequency which leads to higher receptivity.<sup>23,24</sup> While the latter makes use of the stronger  $^1\text{H}$ - $^{15}\text{N}$  and  $^1\text{H}$ - $^{17}\text{O}$  dipolar couplings to improve the overall efficiency of polarization transfer between the  $^{15}\text{N}$  and  $^{17}\text{O}$  nuclei.

Efficient and inexpensive isotopic enrichment of oxygen is one of the major hurdles to wide application of  $^{17}\text{O}$  solid-state NMR spectroscopy for the study of proteins. Fortunately, there has been tremendous recent progress in that area of research.<sup>25-28</sup> As these methods develop further and become routine, and ever higher magnetic fields become accessible, high-resolution NMR experiments incorporating  $^{17}\text{O}$  nuclei such as those presented here are expected to become an indispensable tool for structural biology in addition to the existing arsenal of  $^1\text{H}/^{13}\text{C}/^{15}\text{N}$  pulse sequences.

This work was supported by the National High Magnetic Field Laboratory (NHMFL, USA) through NSF DMR-1644779 and the State of Florida. In addition, we acknowledge the support of the National Institutes of Health through grants AG058504, GM132997 and



GM132079 to RGG. Use of the NHMFL NMR facility is available free of charge; for more information please visit <https://nationalmaglab.org/user-facilities/nmr-mri>.

## REFERENCES

- (1) Wu, G. Solid-State  $^{17}\text{O}$  NMR Studies of Organic and Biological Molecules. *Prog. Nucl. Magn. Reson. Spectrosc.* **2008**, *52* (2–3), 118–169. <https://doi.org/10.1016/j.pnmrs.2007.07.004>.
- (2) Paulino, J.; Yi, M.; Hung, I.; Gan, Z.; Wang, X.; Chekmenev, E. Y.; Zhou, H.-X.; Cross, T. A. Functional Stability of Water Wire-Carbonyl Interactions in an Ion Channel. *Proc. Natl. Acad. Sci. U. S. A.* **2020**, *117* (22), 11908–11915. <https://doi.org/10.1073/pnas.2001083117>.
- (3) Barbet-Massin, E.; Pell, A. J.; Retel, J. S.; Andreas, L. B.; Jaudzems, K.; Franks, W. T.; Nieuwkoop, A. J.; Hiller, M.; Higman, V.; Guerry, P.; Bertarello, A.; Knight, M. J.; Felletti, M.; Le Marchand, T.; Kotelovica, S.; Akopjana, I.; Tars, K.; Stoppini, M.; Bellotti, V.; Bolognesi, M.; Ricagno, S.; Chou, J. J.; Griffin, R. G.; Oschkinat, H.; Lesage, A.; Emsley, L.; Herrmann, T.; Pintacuda, G. Rapid Proton-Detected NMR Assignment for Proteins with Fast Magic Angle Spinning. *J. Am. Chem. Soc.* **2014**, *136* (35), 12489–12497. <https://doi.org/10.1021/ja507382j>.
- (4) Penzel, S.; Smith, A. A.; Agarwal, V.; Hunkeler, A.; Org, M.-L.; Samoson, A.; Böckmann, A.; Ernst, M.; Meier, B. H. Protein Resonance Assignment at MAS Frequencies Approaching 100 KHz: A Quantitative Comparison of J-Coupling and Dipolar-Coupling-Based Transfer Methods. *J. Biomol. NMR* **2015**, *63* (2), 165–186. <https://doi.org/10.1007/s10858-015-9975-y>.
- (5) Hung, I.; Keeler, E. G.; Mao, W.; Gor'kov, P. L.; Griffin, R. G.; Gan, Z. Residue-Specific High-Resolution  $^{17}\text{O}$  Solid-State Nuclear Magnetic Resonance of Peptides: Multidimensional Indirect  $^1\text{H}$  Detection and Magic-Angle Spinning. *J. Phys. Chem. Lett.* **2022**, *13* (28), 6549–6558. <https://doi.org/10.1021/acs.jpcclett.2c01777>.
- (6) Paulson, E. K.; Morcombe, C. R.; Gaponenko, V.; Dancheck, B.; Byrd, R. A.; Zilm, K. W. Sensitive High Resolution Inverse Detection NMR Spectroscopy of Proteins in the Solid State. *J. Am. Chem. Soc.* **2003**, *125* (51), 15831–15836. <https://doi.org/10.1021/ja037315+>.
- (7) Chevelkov, V.; van Rossum, B. J.; Castellani, F.; Rehbein, K.; Diehl, A.; Hohwy, M.; Steuernagel, S.; Engelke, F.; Oschkinat, H.; Reif, B.  $^1\text{H}$  Detection in MAS Solid-State NMR Spectroscopy of Biomacromolecules Employing Pulsed Field Gradients for Residual Solvent Suppression. *J. Am. Chem. Soc.* **2003**, *125* (26), 7788–7789. <https://doi.org/10.1021/ja029354b>.
- (8) Meier, B. H. Cross Polarization under Fast Magic Angle Spinning - Thermodynamical Considerations. *Chem. Phys. Lett.* **1992**, *188* (3–4), 201–207.
- (9) Carroll, P. J.; Stewart, P. L.; Opella, S. J. Structures of Two Model Peptides: N-Acetyl-D,L-Valine and N-Acetyl-L-Valyl-L-Leucine. *Acta Crystallogr. C Cryst. Struct. Commun.* **1990**, *46* (2), 243–246. <https://doi.org/10.1107/S0108270189004762>.

- (10) Frydman, L.; Harwood, J. S. Isotropic Spectra of Half-Integer Quadrupolar Spins from Bidimensional Magic-Angle-Spinning NMR. *J. Am. Chem. Soc.* **1995**, *117* (19), 5367–5368.
- (11) Guo, H.; Karplus, M. Ab Initio Studies of Hydrogen Bonding of N-Methylacetamide: Structure, Cooperativity, and Internal Rotational Barriers. *J. Phys. Chem.* **1992**, *96* (18), 7273–7287. <https://doi.org/10.1021/j100197a027>.
- (12) Case, D. A. Calculations of NMR Dipolar Coupling Strengths in Model Peptides. *J. Biomol. NMR* **1999**, *15* (2), 95–102. <https://doi.org/10.1023/A:1008349812613>.
- (13) Yao, L.; Vögeli, B.; Ying, J.; Bax, A. NMR Determination of Amide N–H Equilibrium Bond Length from Concerted Dipolar Coupling Measurements. *J. Am. Chem. Soc.* **2008**, *130* (49), 16518–16520. <https://doi.org/10.1021/ja805654f>.
- (14) Gan, Z. Measuring Multiple Carbon-Nitrogen Distances in Natural Abundant Solids Using R-RESPDOR NMR. *Chem. Commun.* **2006**, No. 45, 4712–4714. <https://doi.org/10.1039/b611447d>.
- (15) Mueller, K. T.; Jarvie, T. P.; Aurentz, D. J.; RobertS, B. W. The REDOR Transform: Direct Calculation of Internuclear Couplings from Dipolar-Dephasing NMR Data. *Chem. Phys. Lett.* **1995**, *242* (6), 535–542. [https://doi.org/10.1016/0009-2614\(95\)00773-W](https://doi.org/10.1016/0009-2614(95)00773-W).
- (16) Lu, X.; Lafon, O.; Trébosc, J.; Amoureux, J.-P. Detailed Analysis of the S-RESPDOR Solid-State NMR Method for Inter-Nuclear Distance Measurement between Spin-1/2 and Quadrupolar Nuclei. *J. Magn. Reson.* **2012**, *215*, 34–49. <https://doi.org/10.1016/j.jmr.2011.12.009>.
- (17) Ishii, Y.; Terao, T.; Hayashi, S. Theory and Simulation of Vibrational Effects on Structural Measurements by Solid-State Nuclear Magnetic Resonance. *J. Chem. Phys.* **1997**, *107* (8), 2760–2774. <https://doi.org/10.1063/1.474633>.
- (18) Wu, G. Solid-State  $^{17}\text{O}$  NMR Studies of Organic and Biological Molecules: Recent Advances and Future Directions. *Solid State Nucl. Magn. Reson.* **2016**, *73*, 1–14. <https://doi.org/10.1016/j.ssnmr.2015.11.001>.
- (19) Wu, G.  $^{17}\text{O}$  NMR Studies of Organic and Biological Molecules in Aqueous Solution and in the Solid State. *Prog. Nucl. Magn. Reson. Spectrosc.* **2019**, *114–115*, 135–191. <https://doi.org/10.1016/j.pnmrs.2019.06.002>.
- (20) Hung, I.; Uldry, A.-C.; Becker-Baldus, J.; Webber, A. L.; Wong, A.; Smith, M. E.; Joyce, S. A.; Yates, J. R.; Pickard, C. J.; Dupree, R.; Brown, S. P. Probing Heteronuclear  $^{15}\text{N}$ – $^{17}\text{O}$  and  $^{13}\text{C}$ – $^{17}\text{O}$  Connectivities and Proximities by Solid-State NMR Spectroscopy. *J. Am. Chem. Soc.* **2009**, *131* (5), 1820–1834. <https://doi.org/10.1021/ja805898d>.
- (21) Antzutkin, O. N.; Iuga, D.; Filippov, A. V.; Kelly, R. T.; Becker-Baldus, J.; Brown, S. P.; Dupree, R. Hydrogen Bonding in Alzheimer’s Amyloid- $\beta$  Fibrils Probed by  $^{15}\text{N}/^{17}\text{O}$  REAPDOR Solid-State NMR Spectroscopy. *Angew. Chem. Int. Ed.* **2012**, *51* (41), 10289–10292. <https://doi.org/10.1002/anie.201203595>.
- (22) Wei, J.; Antzutkin, O. N.; Filippov, A. V.; Iuga, D.; Lam, P. Y.; Barrow, M. P.; Dupree, R.; Brown, S. P.; O’Connor, P. B. Amyloid Hydrogen Bonding Polymorphism Evaluated by  $^{15}\text{N}\{^{17}\text{O}\}$  REAPDOR Solid-State NMR and Ultra-High Resolution Fourier Transform Ion Cyclotron Resonance Mass Spectrometry. *Biochemistry* **2016**, *55* (14), 2065–2068. <https://doi.org/10.1021/acs.biochem.5b01095>.
- (23) Zhou, D. H.; Shah, G.; Cormos, M.; Mullen, C.; Sandoz, D.; Rienstra, C. M. Proton-Detected Solid-State NMR Spectroscopy of Fully Protonated Proteins at 40 KHz Magic-

- Angle Spinning. *J. Am. Chem. Soc.* **2007**, *129* (38), 11791–11801.  
<https://doi.org/10.1021/ja073462m>.
- (24) Böckmann, A.; Ernst, M.; Meier, B. H. Spinning Proteins, the Faster, the Better? *J. Magn. Reson.* **2015**, *253*, 71–79. <https://doi.org/10.1016/j.jmr.2015.01.012>.
- (25) Seyfried, M. S.; Lauber, B. S.; Luedtke, N. W. Multiple-Turnover Isotopic Labeling of Fmoc- and Boc-Protected Amino Acids with Oxygen Isotopes. *Org. Lett.* **2010**, *12* (1), 104–106. <https://doi.org/10.1021/ol902519g>.
- (26) Keeler, E. G.; Michaelis, V. K.; Colvin, M. T.; Hung, I.; Gor'kov, P. L.; Cross, T. A.; Gan, Z.; Griffin, R. G.  $^{17}\text{O}$  MAS NMR Correlation Spectroscopy at High Magnetic Fields. *J. Am. Chem. Soc.* **2017**, *139* (49), 17953–17963.  
<https://doi.org/10.1021/jacs.7b08989>.
- (27) Métro, T.-X.; Gervais, C.; Martinez, A.; Bonhomme, C.; Laurencin, D. Unleashing the Potential of  $^{17}\text{O}$  NMR Spectroscopy Using Mechanochemistry. *Angew. Chem. Int. Ed.* **2017**, *56* (24), 6803–6807. <https://doi.org/10.1002/anie.201702251>.
- (28) Ha, M.; Nader, S.; Pawsey, S.; Struppe, J.; Monette, M.; Mansy, S. S.; Boekhoven, J.; Michaelis, V. K. Racing toward Fast and Effective  $^{17}\text{O}$  Isotopic Labeling and Nuclear Magnetic Resonance Spectroscopy of N-Formyl-MLF-OH and Associated Building Blocks. *J. Phys. Chem. B* **2021**, *125* (43), 11916–11926.  
<https://doi.org/10.1021/acs.jpcc.1c07397>.